366

Egypt. J. Chem. **Vol. 63,** No. 11 pp. 4645 - 4657 (2020)

Egyptian Journal of Chemistry

http://ejchem.journals.ekb.eg/

Influence of Polymers Loaded with ZnO and TiO$_2$ Nanoparticles on Thermal Resistance of Archaeological Wood

Eman Nabil[a]**, Naglaa Mahmoud**[b]**, Ahmed M. Youssef**[c*]**, Samir Kamel**[d]

[a] Cheops Museum, Egypt.

[b] Conservation Department, Faculty of Archaeology, Fayoum University, Egypt.

[c] Packaging Materials Department, National Research Centre, El Behooth St, Dokki - Giza- Egypt.

[d] Cellulose and Paper Department, National Research Centre, El Behooth St., Dokki -Giza- Egypt.

Abstract

The aim of the current study was to examine the efficacy of Regalers 1126, Regalers 1094, and Polyurethane with and without zinc oxide nanoparticles (ZnO-NPs) and titanium oxide nanoparticles (TiO$_2$-NPs) on the thermal resistance of archaeological wood. Cedar and sycamore woods were selected as archaeological woods and aging was performed at 100°C for 400 hours, which is equivalent to 25 years. Fourier transform infrared spectroscopy (FT-IR) was used to study the change in the functional groups. The X-ray analysis (XRD) examined the change of wood crystallization of woods after the consolidation process. Moreover, the changes in the morphology of untreated and treated woods were identified by Scanning Electron Microscopy (SEM). Furthermore, the thermal stability of untreated and treated woods was investigated by thermal gravimetric analysis (TGA). The mechanical decay of treated cedar and sycamore woods by consolidation materials were described. Correspondingly, the color change as indicated by CIE Lab color coordinates of consolidated woods after aging was investigated and the color change rate of sycamore wood is higher than that of cedar wood after the consolidation process. Finally, utilize of TiO$_2$-NPs played a larger role in the weight gain and mechanical properties of samples than ZnO-NPs after the consolidation procedure.

Keywords: Archaeological Wood; Cedar and Sycamore wood; TiO$_2$-NPs; ZnO-NPs; Regalers 1126; Regalers 1094; Polyurethane.

Introduction

Wood Monuments are more susceptible than other monuments to many damage factors that threaten their survival [1]. This is due to the natural defects of the wood by various decay factors and instability of dimensions [2]. Scientists are seeking to find some materials that preserve the quality of such monuments. One of the most important restoration processes is the consolidation process, which is based on the idea of applying artificial products that can penetrate the wood and restore its mechanical properties [3, 4]. While trying to preserve its physical properties, including polymers by impregnating the wood with consolidation materials in this case, the monomers settle in the cell walls and raise their properties [5-7]. However, its exposure to air makes them susceptible to sunlight, moisture and fungal attacks, which weaken their properties as a consolidation agent [8]. In addition, the penetration of monomers is not sufficient to protect wood from various damage factors [9].

Regalers 1126 is a polymer that has the ability to penetrate channels on the walls of cells without affecting wood porosity and altering the behavior of treated wood [1]. While Regalers 1094 has been widely used as an adhesive for glass assembly as well as high ability of saturation, stability and resistance to ultraviolet radiation [10]. Another synthetic polymer is polyurethane which is a water-resistant and weather-protective material. It is also resistant to oxidation and is used to strengthen porous materials such as wood and leather [11].

Nanotechnology technique has been used as one of the most effective techniques for wood protection [12]. Scientists have succeeded in integrating some

_____

polymers with nanomaterial to increase the efficiency of polymers and raise their properties [13-18]. Nanomaterials provide a better treatment method than traditional materials because nanoparticles are easy in penetration, stabilization and distribution by the wood cell walls as well as low viscosity properties [19]. These specifications make it more efficient to raise the properties of wood, beside the new wood behavior such as self-cleaning, pore size minimizing and the volume available for water absorption, which are utilized to overcome wood deficiencies [20, 21]. Due to the efficiency of nanoparticles in raising the properties of polymers, ZnO nanoparticles (ZnO-NPs) were used, where it renders protection to the treated surfaces of damage appearances. It has the potential to inhibit and resist microbiological damage and is given good results as a water inhibitor, oxidative and atmospheric contaminants especially when used with polymer. It is used with polymers to treat dry wood surfaces as it helps to increase polymer penetration of wood with high resistance for moisture, UV and fungus [22-24]. Another nanoparticle is TiO2-NPs, the most commonly used nanomaterial in organic and inorganic processes [25, 26]. By mixing the nanoparticles with the polymer, the polymer is made extra water repellent as well as being able to self-cleaning or self-protection, and improve surface cleaning with increased resistance to various damage factors without any effect on the treated surface, in addition to being nontoxic material [27].

The current study focuses on using Regalers 1126, Regalers 1094, and Polyurethane with/without ZnO-NPs and TiO_2-NPs in the consolidation of thermally damaged wood, and evaluating them as the best wood preservation ability. Cedar and sycamore woods were archaeological woods. By FT-IR a significant change in the functional groups of wood after the consolidation process was studied. While the change of crystallization and crystalline size in woods was investigated by XRD and a resistance of reinforced woods at high temperatures by TGA. The effect of nanoparticles on supporting of the inner cell walls of the wood was examined by SEM.

Materials and Methods
Materials
Cedar wood was imported from Lebanon. Sycamore woods were collected from Egypt. Regalers 1126 and Regalers 1094 of low molecular weight aliphatic resins were imported from Italy. Polyurethane (polyisocyanates polyurethane) was purchased from Egypt. Titanium (IV) isopropoxide, 97% (TTIP), glycerol and nitric acid (HNO_3) were obtained from Sigma-Aldrich chemicals that used to prepare TiO_2-

NPs. Zinc-acetate (puriss, Reanal, Hungary) (Zn(CH3COO)2·2H2O) was used to prepare ZnO-NPs.

Methods
Preparation of ZnO-NPs
In order to fabrication ZnO nanoparticles, stock solutions of $Zn(CH_3COO)_2 \cdot 2H_2O$ (0.2 M) as prepared in 50 ml methanol under stirring. To this stock solution 50 ml of NaOH (varying from 0.4 M to 0.8 M) in methanol was added under constant stirring in order to get the pH value of reactants between 8 and 11. These solutions were transferred into Teflon lined sealed stainless-steel autoclaves and continuous at various temperature in the range of 100–200°C for 12h under autogenously pressure. It was then allowed to cool naturally to room temperature. After the reaction was complete, the resulting white solid products were washed with methanol, filtered and then dried in a laboratory oven at 60°C.

Preparation of TiO_2-NPs
The titanium dioxide nanoparticles (TiO_2-NPs) were prepared using sol-gel technique. This method carried out by the hydrolysis and condensation of titanium tetra isopropoxide (TTIP) which descried by Moustafa *et al.*, [28]. A solution was prepared by dilution of 10 ml of TTIP with 40 mL of isopropanol. Then this solution was added drop wise in distilled water kept at pH 2-3 using conc. HNO_3, stirred for 2 h and heated in a water bath at 60-70 °C for 20 h. The formed TiO_2 nanoparticles were recovered and dried at 100°C.

Preparation of wood samples
Samples of cedar and sycamore woods were prepared as 10 x 1 x 1 cm in dimensions for bending tests, and the preparation of samples of $2 \times 2 \times 2$ cm in dimensions for compression tests as in the physical and chemical tests were conducted on the same samples of the above dimensions.

Wood Treatment
Wood samples were dipped in different polymer solutions for 30 min. These polymers are 5% Regalers 1126 or Regalers 1094 dissolved in white Spirit-toluene mixture (1:1) while 5% Polyurethane dissolved in toluene. After dipping, the wood samples were pressed between two filter paper sheets to remove the excess polymer, and then dried. In another trials 0.75% (wt/ vol) of ZnO-NPs or TiO_2-NPs were added.

Aging
Aging was carried out in the oven for 400 h at 100 °C, which is equivalent to 25 years (archaeological woods). All samples were weighed before and after

_____

_____

heat treatment and the percentage of loss in the mass has been calculated.

Characterization
Measurements of Color change
Color changes caused by the effect of accelerated ageing cycles were measured using CIE L*a*b* system commonly used to compare the colors of two samples. The L* - scale measures lightness, and varies from 0 (black) to 100 (perfect white). The a* - scale measures ed-green; +a* means more red, -a* measures green; the b* - scale measures yellow-blue; +b* meaning more yellow, -b* more blue. The total color difference (ΔE*) is calculated according to the following equation:

In order to determine the chromatic evolution, the deviation was calculated for every coordinate (L*, a* and b*) in rapport with its initial value, on each sample and on the same place. Finally, the total change of colors was calculated in each point, using the above equation. The measurement was made using Ultra Scan PRO Hunter Lab D65, 10A.

Mechanical properties
Bending and compression strengths were measured with a universal testing machine LK10k.

FT-IR analysis
The change in wood functional groups was studied using FT-IR analysis; it was performed using Jasco FT-IR- 6100 spectroscopy with resolution 4 cm^{-1}, and wave number range from 537 cm^{-1} to 4000 cm^{-1}.

X-Ray Diffraction (XRD)
The XRD patterns of untreated and treated wood samples were used to examine the change of wood crystallization of woods after the consolidation process on a Diano X-ray diffractometer using a Cu (Kα1/Kα2) radiation source energized at 45 kV and a Philips X-ray diffractometer (PW 1930 generator, PW 1820 goniometer). The XRD patterns were recorded in a 2θ diffraction angle range from 10° to 80°.

Thermo-gravimetric analysis
Thermogravimetric analysis (TGA) were performed using SDYQ-600 thermal analyzer, on 20 mg samples in the range of 30 to 700°C at a heating rate 10°C/min under inert atmosphere.

Scanning electron microscopy (SEM)
The surface morphology of untreated and treated wood samples was analyzed using scanning electron microscopy (SEM), (JSM 6360LV, JEOL/Japan). The microscope was attached to a dispersive energy spectrometer (EDS). The images were obtained using an accelerating voltage of 10–15 kV. EDX analysis was carried out to be supporting information

confirming the presence of nanoparticles in treated samples.

Transmission electron microscopy (TEM)
The structure and surface morphology of the prepared TiO₂-NPs as well as ZnO-NPs powders were examined via JEOL JEM-1230 transmission electron microscope (TEM) with acceleration voltage of about 80 kV. A small drop of the dispersion of nanoparticles onto a Lacey carbon filmcoated copper grid and allowed to dry initially in air then by applying high vacuum.

Results and Discussion
Structure evaluation of the prepared nanomaterials and its nanocomposites

In this study we selected three consolidation materials; Regalers 1126, Regalers 1094, and Polyurethane with and without ZnO-NPs or TiO₂-NPs as preserving materials for cedar and sycamore woods from thermal damaged. The chemical structure of these preserving materials is shown in (Fig. 1).
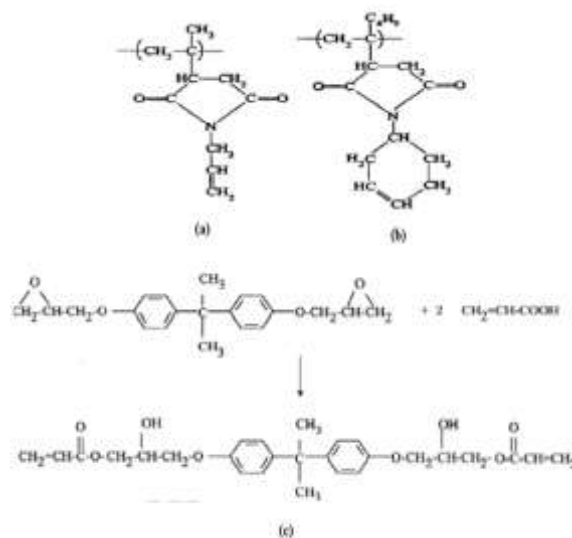
Fig. 1 Chemical structure of (a) Regalers 1126, (b) Regalers 1094, and (c) Polyurethane

In general, nanometals enhance the polymer properties regarding the thermal stability, microbial damage, and water resistance [29]. ZnO-NPs used with polymers to treat dry wood surfaces which help to increase polymer penetration of wood with high resistance for moisture, UV and fungus [30]. TiO₂-NPs have antimicrobial properties and high ability of permeability inside the wood and distribute regularly within the wood walls and raise its mechanical properties [31, 32].

_____

_____
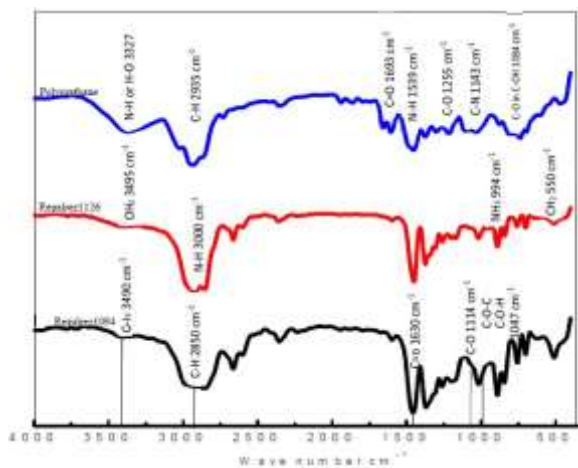
Fig. 2 FT-IR of Regalers 1126, Regalers 1094, and Polyurethane

Figure 2 displayed that the FT-IR of the Regalers 1126, Regalers 1094, and Polyurethane which used as preserving materials for cedar and sycamore woods from thermal damaged. For Regalers 1094 the (O-H) group appears at 3490 cm^{-1}, (C-H) aliphatic appear at 2850 cm^{-1}, (C=O) seem at 1630 cm^{-1} and (C-O) group appear at 1114 cm^{-1}. For Regalers 1126 the (O-H) group appears at 3495 cm^{-1}, (N-H) group look at 3000 cm^{-1}, (NH$_2$) group seem at 994 cm^{-1} and (CH$_2$) group appear at 550 cm^{-1}. While the FT-IR of Polyurethane demonstrated that the (N-H) or (O-H) group at 3372 cm^{-1}, (C-H) aliphatic appear at 2935 cm^{-1}, (C=O) appear at 1693 cm^{-1} (N-H) group look at 1539 cm^{-1}, (C-O) group look at 1255 cm^{-1}, (C-N) group look at 1143 cm^{-1} and (C-OH) group appear at 1084 cm^{-1}

The morphological structure of the prepared TiO$_2$-NPs was examined using X-ray diffraction (XRD), transmission electron microscopy as well as scanning electron microscopy (SEM) apparatuses. The XRD pattern of TiO$_2$-NPs originates to an agreement with the JCPDS card no. 21-1272 (anatase TiO$_2$). Furthermore, the TiO$_2$ in the anatase phase was demonstrated with strong diffraction peaks at 2θ = 25° (101) also the peak at 2 θ = 48° (200). There is no any false diffraction peak existing in the fabricated TiO$_2$-NPs.
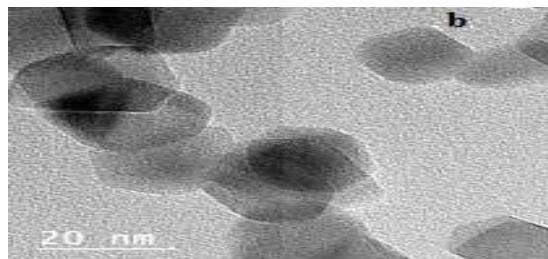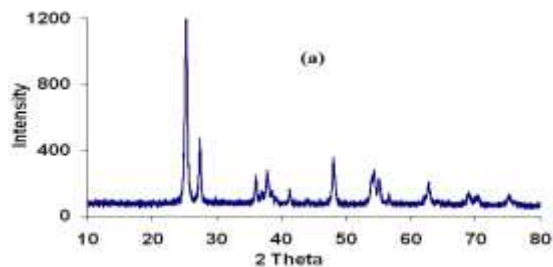
Fig. 3. a) XRD TiO$_2$-NPs and b) TEM image of TiO$_2$-NPs

The intensity of XRD peaks of the sample discloses that the prepared TiO$_2$-NPs are crystalline as well as comprehensive diffraction peaks elect exact small size crystallite. **Fig. 3a** demonstrations the XRD pattern of TiO$_2$-NPs prepared via hydrothermal method, the pattern could be expected to the diffraction of (101), (103), (004), (112), (200), (105) and (211), planes of face centered cubic (fcc) TiO$_2$-NPs as shown in (**Fig. 3a**), which are evidence the establishment of TiO$_2$-NPs, and this is associated with TEM interpretations [33]. Moreover, the TEM evaluations were carried out to study the surface structure of the fabricated TiO$_2$-NPs which presented the creation of the TiO$_2$ nanoparticles and the particles have diameters less than 25 nm as revealed in (**Fig. 3b**). For studying the morphological properties of the fabricated ZnO-NPs, transmission electron microscope (TEM) images were carried out examine the crystalline ZnO-NPs which synthesized using a solvothermal method.

TEM image proves the construction of ZnO-NPs and the size of their particles with an average size from 8 to 15 nm as shown in (**Fig. 4b**). Correspondingly, the XRD patterns of ZnO-NPs are displayed in (**Fig. 4a**). The XRD profile of ZnO-NPs presented characteristic peaks equivalent to the planes (1 0 0) at 2θ = 31.7°, also the plane (0 0 2) at 2θ = 34.4°, (1 0 1) at 2θ = 36.25°, (1 0 2) at 2θ=47.5°, (1 1 0) at 2θ = 56.6°, (1 0 3) at 2θ = 62.8° and (1 1 2) at 2θ = 66.3°. This XRD pattern displays that the fabrication of ZnO-NPs leads to

_____

_____

quartzite phase besides all the diffraction peaks reach agreement with the described JCPDS data. This was established with TEM results, in which ZnO-NPs seem as spherical particles with size around 8 to 15 nm as shown in (**Fig. 4a**).
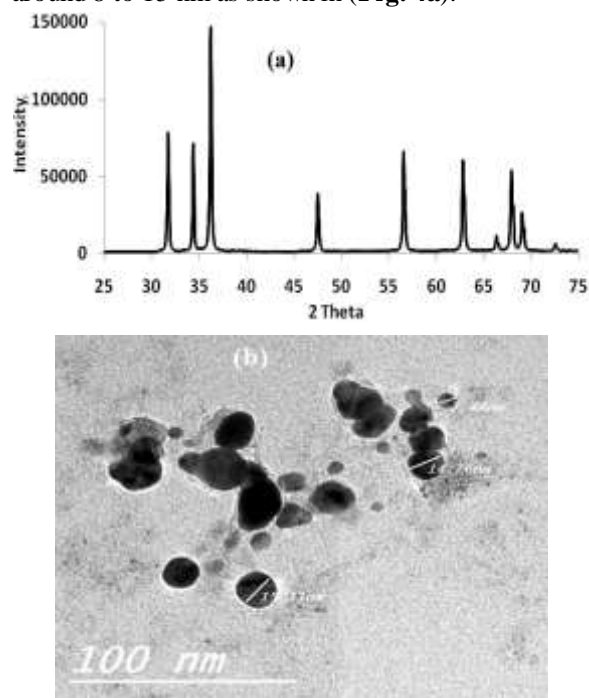
Fig. 4: a) XRD and b) TEM image of ZnO-NPs

Color change measurement

Preserving the physical properties of wood after the consolidation process is important to be studied to evaluate the efficiency of the consolidation material in achieving the desired objective. The color change device records four readings for each sample (ΔE - b* - a* L*) L* records the color gradient coordinate from black to white in transition from (0:100), b* records the color gradient coordinate of the yellow in the positive direction to the blue in the negative

direction. a* records the color gradient coordinate of the red in the positive direction to green in the negative direction [34]. ΔE is the average of the three readings (b* - a* - L*). The color change of sycamore wood was higher than that of cedar wood after the consolidation process. There was no significant color change of samples after consolidation by polymerization and with nanoparticles as opposed to using polymers only. TiO$_2$-NPs combined with the Regalers 1094 gave the best results with cedar wood. Whereas the best results were gained with polyurethane when was applied with sycamore wood. **Table 1** and (**Fig. 5a &b**) displays the difference between the rates of color change of wood after treatment without/with nanomaterials.
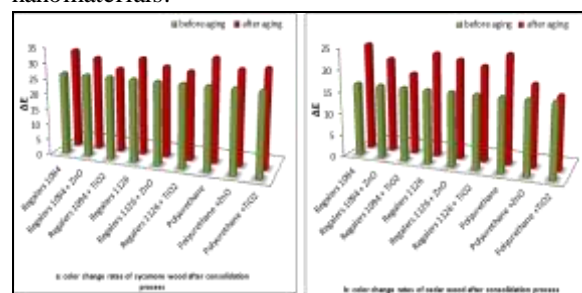
Fig. 5. Difference between color change rates of sycamore and Cedar wood, after consolidation process

Weight percent gain

In wood consolidation process by polymeric materials, increasing in the weight of wood indicates the extent of the penetration of the consolidation materials and the wood absorbance

Table: 1 Coloration measurements of untreated and treated cedar and sycamore woods by consolidation materials

Consolidation material	Sycamore Wood				Cedar Wood			
	L*	a*	b*	ΔE	L*	a*	b*	ΔE
Untreated	0.0630	10.37	15.90	27.00	17.00	17.00	17.00	17.00
Regalers 1094	32.90	10.78	16.80	33.00	34.57	12.70	21.01	25.00
Regalers 1094/ZnO-NPs	30.20	11.60	15.80	31.00	19.80	11.66	34.56	22.00
Regalers 1094/TiO$_2$-NPs	36.77	11.30	18.34	28.00	35.50	11.27	17.70	19.00
Regalers 1126	36.,88	12.00	14.54	32.00	29.06	10.,04	30.39	24.00
Regalers 1126/ZnO-NPs	34.05	12.44	21.64	30.00	36.11	11.79	19.37	23.00
Regalers 1126/TiO$_2$-NPs	35.20	10.90	17.30	29.00	36.11	11.17	21.72	22.00
Polyurethane	29.19	20.84	12.,23	34.00	18.12	11.56	33.94	25.00
Polyurethane/ ZnO-NPs	32.30	12.70	21.19	31.00	21.47	11.65	39.60	19.00
Polyurethane/ TiO$_2$-NPs	30.88	20.84	12.23	32.00	24.48	12.25	45.27	17.00

_____

thereof. **Fig. 6** demonstrations the rate of increasing the weight of cedar and sycamore woods after consolidation by Regalers 1126, Regalers 1094, and Polyurethane with and without nanomaterials (ZnO-NPs and TiO$_2$-NPs). It is clear from the (**Fig. 6**) that, the nanomaterials enhance the rate of weight increasing with three consolidation materials this means that nanomaterials could permeate the wood. The rate of permeation of TiO$_2$-NPs is higher than that of ZnO-NPs, this is reflected positively on the strength of wood. Also, the rate of weight increasing with sycamore is higher than that of cedar wood with and without nanomaterials.
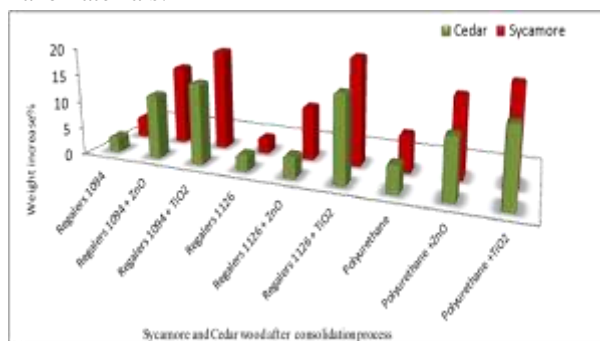
Fig. 6 The average weight increase in Sycamore and Cedar wood after consolidation process

Mechanical measurements

Fig. 7 displays the change in bending and compression resistances for all samples under test. The bending and compression resistances after treatment of cedar and sycamore woods by consolidation materials show the following order: Regalers 1126/ TiO$_2$-NPs > Regalers 1094/ TiO$_2$-NPs > Polyurethane/ TiO$_2$-NPs > Regalers 1126/ ZnO-NPs > Regalers 1094/ ZnO-NPs > Polyurethane/ ZnO-NPs > Polyurethane > Regalers 1094 > Regalers 1126 this order can be related to the characterization nature of each polymeric materials and nanometer materials increase the efficiency of these materials. From these results we can concluded that the using of thesis consolidation materials improved the mechanical properties of cedar and sycamore woods which agreement with increasing of woods weights.
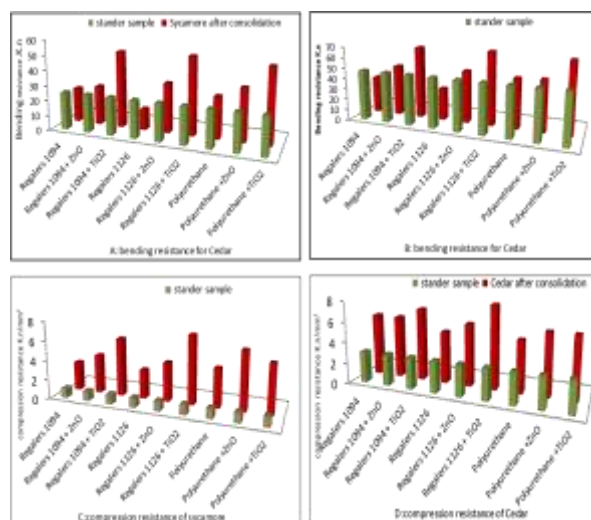
Fig. 7 Bending and compression resistances of untreated and treated cedar and sycamore woods by consolidation materials

Infrared Analysis (FTIR)

All types of wood have common features in the FT-IR spectra where a vibration area at 2500 - 3500 cm^{-1} is characteristic to water part (O-H) [35]. A vibration area for (C-H Stretching) at 600: 1800 cm^{-1} for cellulose and 1724 -1736 cm^{-1} is a specific of (C-O) group of hemicellulose, while 1594 - 1602 cm^{-1} for (C-O) group of the total content of the lignin. Significant changes in the FT-IR spectra were obtained after consolidation process and aging in the region comprised of bands assigned to the main components of wood: cellulose, hemicellulose, and lignin. **Fig. 7a&b** illustrates the FT-IR spectra of untreated and treated cedar and sycamore woods by consolidation materials.

From (**Fig. 8a, b**) the largest extension of the hydroxyl group (OH Stretching) has shown up after the conductance of consolidation materials with nanomaterials. A significant shrinkage also was observed in the carbonyl group (C=O) and the ether absorbance group (C-O) in wood after the consolidation process on all samples. In addition, polymer functional groups appeared in extension of the wood after the consolidation process. In addition, the magnitude of the peak decreased with loading nanoparticles and aging.

_____

_____
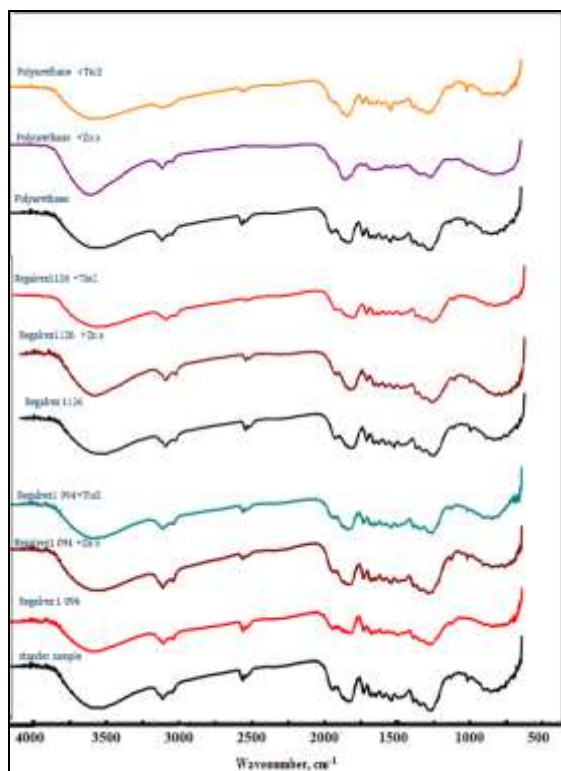
Fig. 8a FT-IR spectra of untreated and treated sycamore wood by consolidation materials
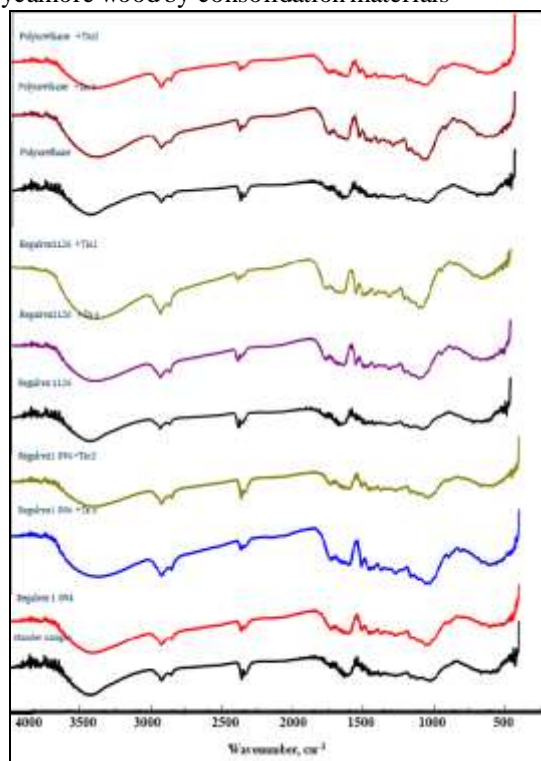
Fig. 8b FT-IR spectra of untreated and treated cedar wood by consolidation materials

X-ray diffraction (XRD)

The most common method to obtain structural characteristic changes is XRD, as it gives information about crystal size. Table 2 shows the change in crystallization of cellulose in sycamore and cedar woods after the consolidation process. From the table it is clear that there was a significant change in the crystallization degree.

Table 2 Degree of crystallization of cellulose in sycamore and cedar woods before and after consolidation process

Consolidation material	Cedar	Sycamore
Untreated	29.85	26
Regalrez1094	15	14
Regalrez1094/ ZnO-NPs	30	15
Regalrez1094/ TiO$_2$-NPs	33	35
Regalrez1126	30	22
Regalrez1126/ ZnO-NPs	40	37
Regalrez1126/ TiO$_2$-NPs	41	46
Polyurethane	30	20
Polyurethane/ ZnO-NPs	36	18
Polyurethane/ TiO$_2$-NPs	37	30

Fig. 9 Shows the X-RD of untreated and treated cedar and sycamore woods with consolidation materials. For all samples two peaks appeared at $2\theta \sim 18$ and 23 referred to the amorphous part and crystalline region of cellulose respectively. The XRD study of consolidated woods with TiO$_2$-NPs presented one diffractogeam with one peak at 24° which correlated to crystal lattice of TiO$_2$-NPs loaded into consolidated woods (Fig. 9). It shows that ZnO-NPs have a strong peak at 37:30 (2θ) with Regalers 1126 and polyurethane but a week peak with Regalers 1094. At 22:20 (2θ) of TiO$_2$-NPs appeared with treated with all consolidation materials.
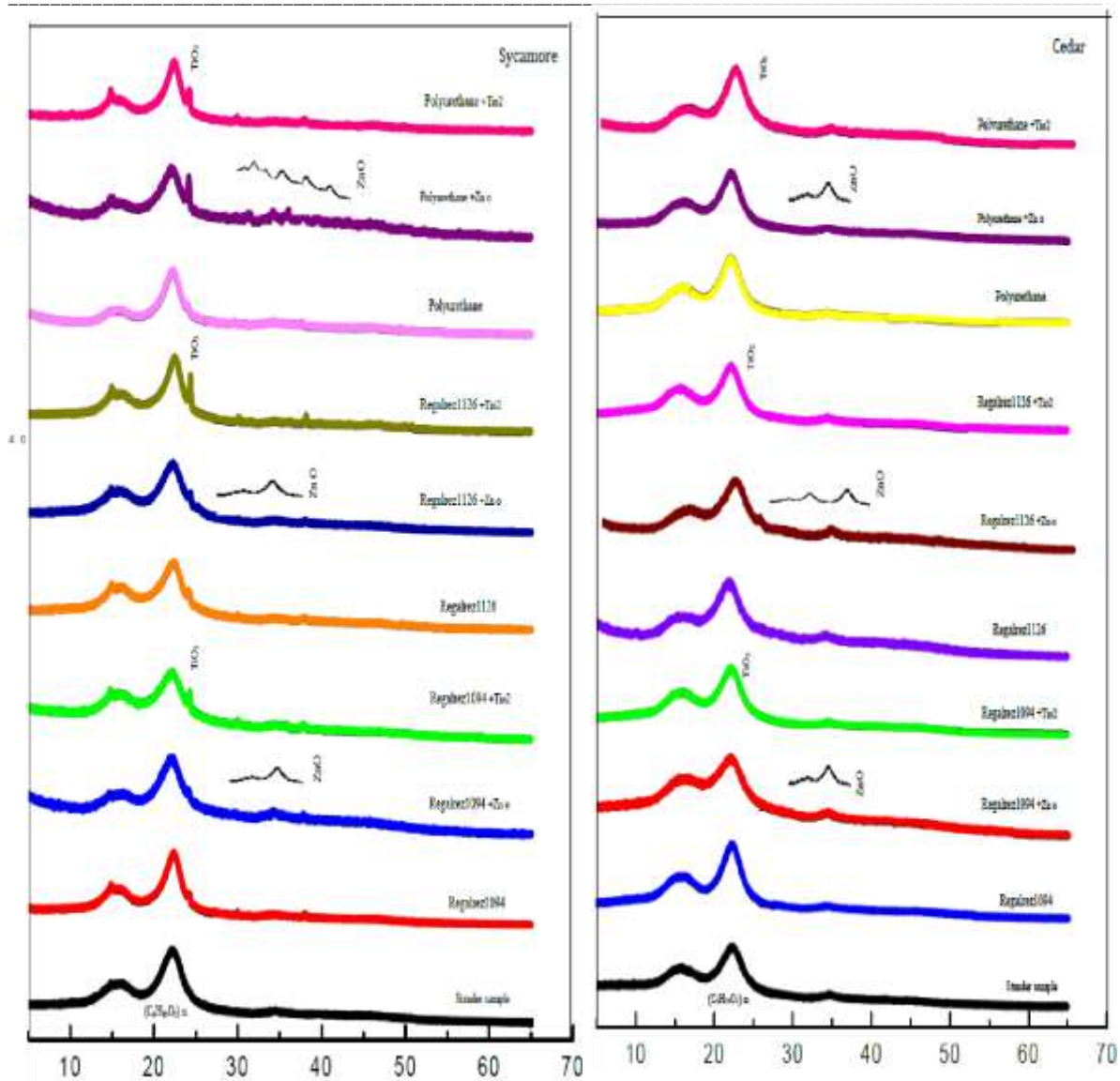
_____

_____

Fig. 9 X-RD of untreated and treated cedar and sycamore woods by consolidation materials

_____

INFLUENCE OF POLYMERS LOADED WITH ZNO AND TIO$_2$ NANOPARTICLES..

4653
_____

Thermal analysis (TGA)

The mass reduction curve of the samples was measured after the consolidation process to study the effect of wood consolidation materials when exposed to different temperatures. Fig. 10 shows the mass reduction curve of the woods in three phases. Phase one < 250 °C; with no effect on the mass of wood, with only the loss of the free water [36]. Phase two 250:350°C; the degree of polymerization is reduced, and as a result of high temperature, hydrogen bonds get cracking, leading in the separation of structural units to small units resulting in the decomposition of both of cellulose and hemicellulose, which are the basic components of wood (62) followed by a significant reduction in weight [37]. Phase three 400:

500 °C; degradation of wood components, especially lignin. Lignin is found between cells and inside walls and binds cells to each other, which is the most stable component when exposed to heat. At high temperatures, lignin degrades leading to wood collapse and loss of weight, the last phase of thermal decomposition [38]. By comparing the mass reduction curve for both standard and reinforced samples of sycamore and cedar woods, it was found that Regalers 1126/ ZnO-NPs were more stable at high temperatures as the addition of ZnO-NPs to polymers improved wood properties in terms of stability at high temperatures

Scanning electron microscopy (SEM)
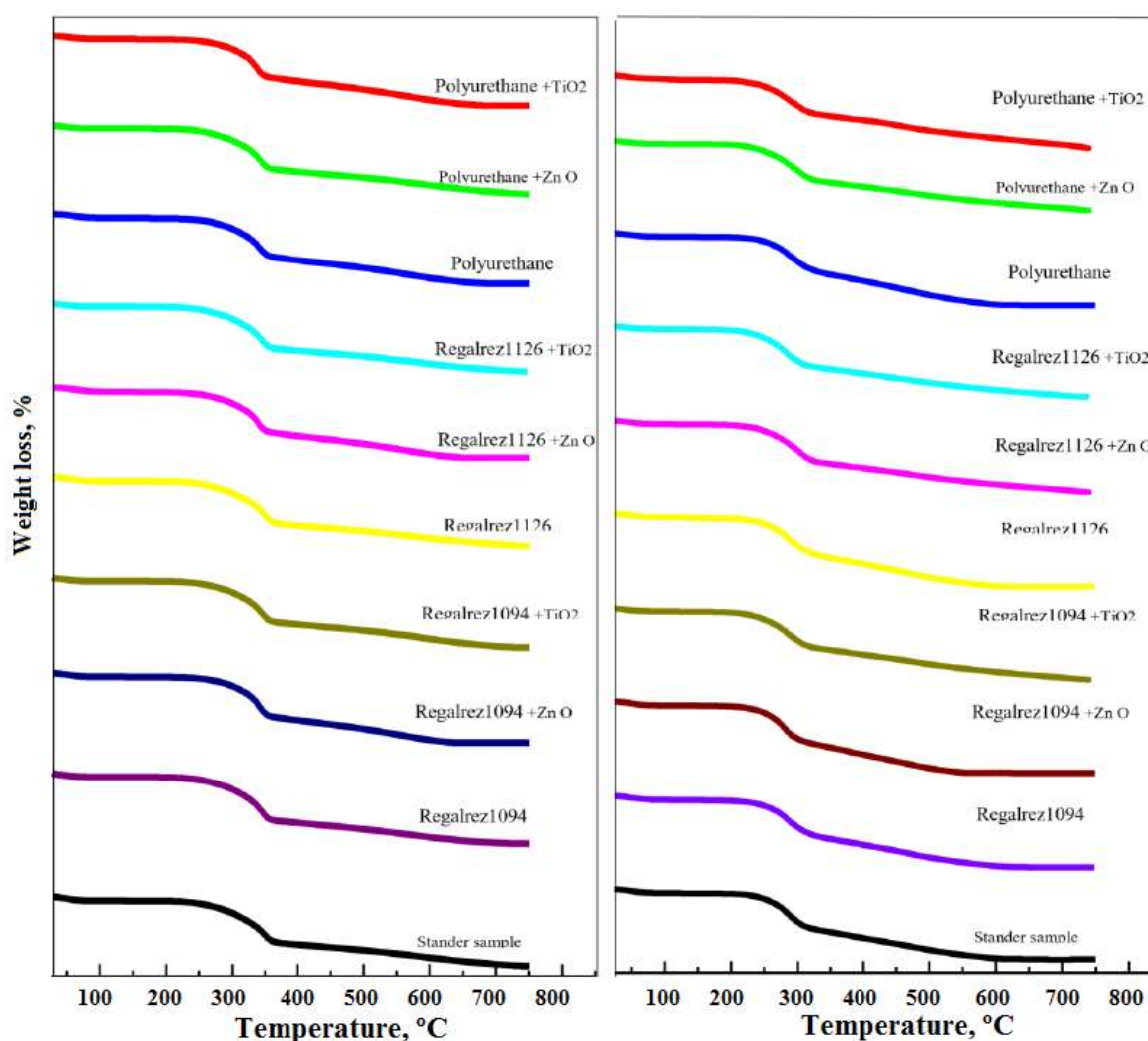
Fig. 10. TGA of untreated and treated cedar and sycamore woods by consolidation materials

_____

_____

Fig. (11a, b) displays the SEM micrographs of untreated and treated wood samples. The empty cell wall and pits were observed in untreated wood. In treated wood, these empty spaces were occupied by the polymers. The impregnated nanoparticles were located in the wood. It can be observed, nanoparticles were nearly homogeneously dispersed in the woods. There also were nearly uniformity in the distribution of nanoparticles in the treated woods and no aggregation of nanoparticles observed. So, we can conclude that there has been a significant improvement in the consolidation of the cell walls with the reinforced samples, especially when the nanoparticles are used, where the nanometer grains settle in the internal spaces of the cells and act as a support as well as filler [39]. After the microscopic examination of the samples (**Fig. 11a, b**), we found the best supporting material to support the inner walls of the wood is Regalers 1126/ ZnO-NPs
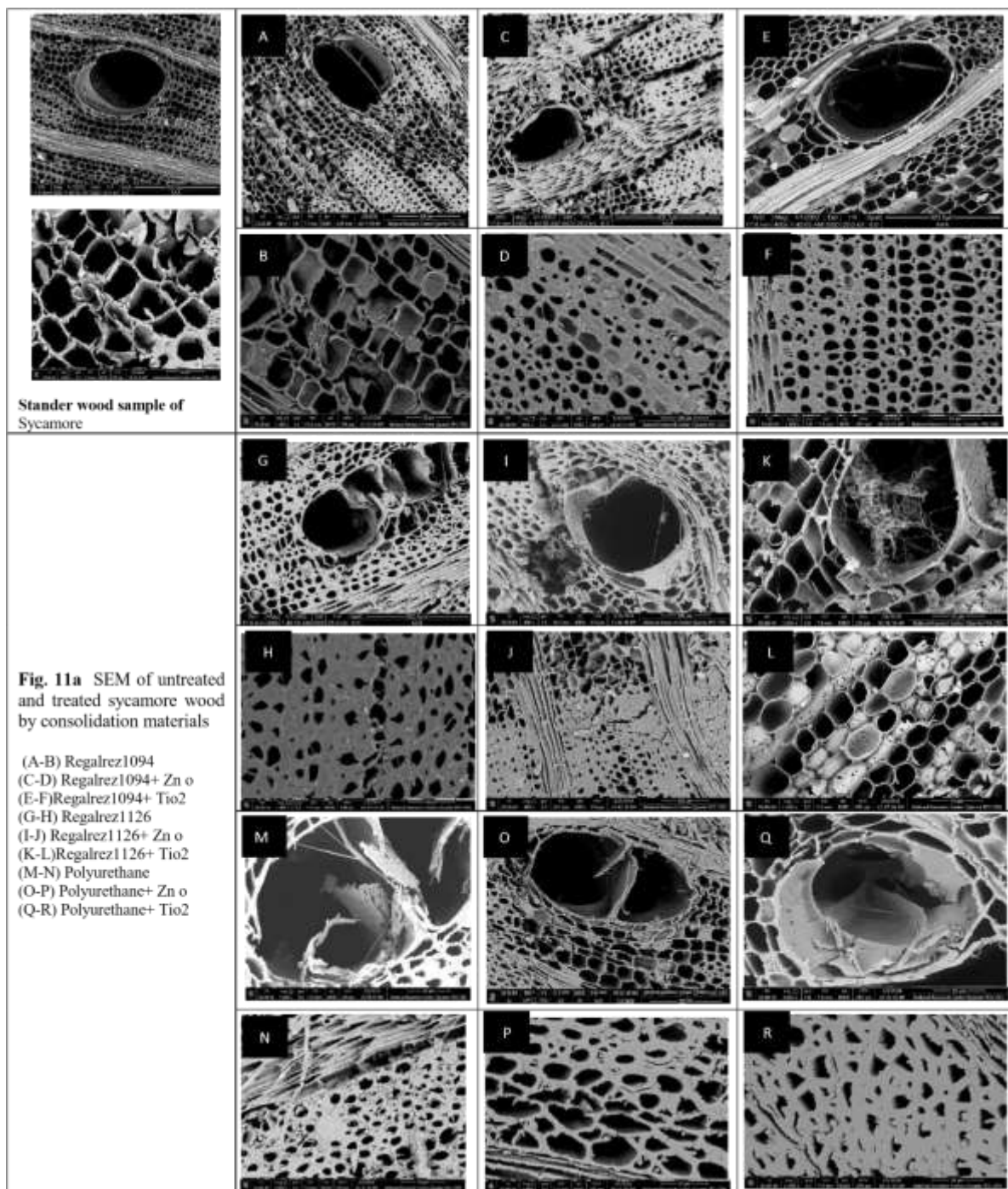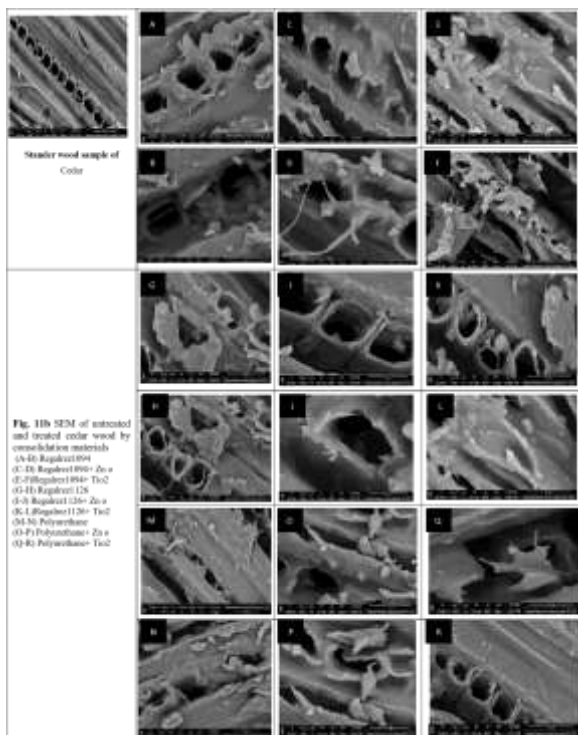
Stander wood sample of Sycamore

Fig. 11a SEM of untreated and treated sycamore wood by consolidation materials

(A-B) Regalrez1094
(C-D) Regalrez1094+ Zn o
(E-F)Regalrez1094+ Tio2
(G-H) Regalrez1126
(I-J) Regalrez1126+ Zn o
(K-L)Regalrez1126+ Tio2
(M-N) Polyurethane
(O-P) Polyurethane+ Zn o
(Q-R) Polyurethane+ Tio2

_____

_____

Fig. 11b SEM of untreated
and treated cedar wood by
consolidation materials
(A-B) Regalrez1094
(C-D) Regalrez1094+ Zn o
(E-F)Regalrez1094+ Tio2
(G-H) Regalrez1126
(I-J) Regalrez1126+ Zn o
(K-L)Regalrez1126+ Tio2
(M-N) Polyurethane
(O-P) Polyurethane+ Zn o
(Q-R) Polyurethane+ Tio2

Conclusion

- In this work we introduced a new idea as ZnO-NPs and TiO$_2$-NPs were incorporated into Regalers 1126, Regalers 1094, and Polyurethane.

- SEM imaging for the treated wood samples showed the nanoparticles are stabilized in the inner spaces of the wood, and supporting them.

- The color change rate of sycamore wood is higher than that of cedar wood after the consolidation process.

- TiO$_2$-NPs played a larger role in the weight gain and mechanical properties of samples than ZnO-NPs after the consolidation process.

- In general, the efficiency of the consolidation material depends on the type and condition of the wood.

Conflict of interests

The authors declare that they have no conflict of interests.

Acknowledgements

References

1. Glinchey CW (1990) "The industrial use and development of low molecular weight resins: an examination of new products of interest to the conservation field; ICOM Committee for Conservation. (II), 563-567

2. Baysal E, Kart S, Toker H, Degirmentepe S (2014) Some physical characteristics of thermally modified oriental-birch wood, Ciencia y tecnología 16(3): 291-298.

3. Mantanis GI, Papadopoulos A N. (2010): Reducing the thickness swelling of wood-based panels by applying a nanotechnology compound. Eur. J. of Wood and Wood Prod. (68), 237-239

4. Youssef, A. M., El-Gendy, A., Kamel S. Evaluation of corn husk fibers reinforced recycled low density polyethylene composites. Materials Chemistry and Physics, 152(2015) 26–33.

5. Crisci M, La Russa MF, Malagodi M, Ruffolo SA (2010) Consolidating properties of Regalrez 1126 and Paraloid B72 applied to wood Gino Journal of Cultural Heritage 11(3) 304-308.

6. Dilek S, Olgun G (1995) Radiation initiated copolymerization of allyl 2 3 epoxy propyl ether with acrylonitrile and methyl methacrylate and their potential use in the preservation of wooden objects, Radiation Physics and Chemistry (46) 889–892

7. Rushdy, A. M., Wahba, W. N., Youssef, A. M., and Kamel S. (2017). Influence of Bleaching Materials on Mechanical and Morphological Properties for Paper Conservation, Egypt. J. Chem.Vol. 60, No. 5, pp.893 - 903

8. Schniewind AP, Eastman PY (1994) Consolidant distribution in deteriorated wood treated with soluble resins, Journal of the American Institute for Conservation

9. Castelli C, Gigli MC, Lalli C, Lanterna G, Weiss C, Speranza L (2002) Un compost organico sintetico per il consolidamento del legno: sperimentazione, misure eprime applicazioni, OPD restauro (22) 144–152.

10. Clausi M, Crisci GM, La Russa M.F, Malagodi M, Palermo AM, Ruffolo SA (2009) Studio degli effetti prodotti da funghi da carie bianca e bruna su legno trattato con prodotti consolidanti", Convegno "Scienza e Beni Culturali" Bressanone, 45 (3). 465-474

11. Chapman S, Mason D (2003) The use of Paraloid B72 as a surface consolidant for stained glass, Journal of the American Institute for Conservatio ,42, 381–392.

_____

_____

12. Habibzade1S, Omidvar1 A, Reza M, Farahani1 M, Mashkour M (2014), Effect of NanoZnO on Decay Resistance and Artificial Weathering of Wood Polymer Composite Journal of Nanomaterials &Molecular Nanotechnology 3(3) p2-5.

13. El-Sayed, S. M., El-Sayed, H. S., Ibrahim, O. A., & Youssef, A. M. (2020). Rational design of chitosan/guar gum/zinc oxide bionanocomposites based on Roselle calyx extract for Ras cheese coating. Carbohydrate Polymers, 116234.

14. Youssef, A. M. Abou-Yousef, H. El-Sayed, S., Kamel S. (2015) Mechanical and antibacterial properties of novel high performance chitosan/nanocomposite films. International Journal of Biological Macromolecules, 76, 25–32.

15. Abd El-Ghaffar, M.A., Youssef, A.M., Abd El-Hakim A.A. (2015) Polyaniline Nanocomposites via In-situ Emulsion Polymerization based on Montmorillonite; preparation & characterization, Arabian Journal of Chemistry, 8, 771–779

16. Youssef, A.M., Abdel-Aziz, M., El-Sayed, S. (2014). Chitosan Nanocomposite Films Based on Ag-NP and Au-NP Biosynthesis by Bacillus Subtilis as Packaging Material, International Journal of Biological Macromolecules, 69, 185–191.

17. Youssef, A. M., Assem, F. M., Abdel-Aziz, M. E., Elaaser, M., Ibrahim, O. A., Mahmoud, M., & Abd El-Salam, M. H. (2019). Development of bionanocomposite materials and its use in coating of Ras cheese. *Food chemistry*, *270*, 467-475.

18. Youssef, A.M., Malhat, F.M., Abdel Hakim, A.A., Dekany, I. Synthesis and utilization of poly (methylmethacrylate) nanocomposites based on modified montmorillonite. Arabian Journal of Chemistry, 2017, 10(5), pp. 631-642

19. Meilert KT, Loub D, Kiwi J (2005) Photocatalytic self-cleaning of modified cotton textiles by TiO2 clusters attached by chemical spacers. J Mol Catal A: Chem 2(37) 101–108

20. Kathiervelu SS (2003) Applications of nanotechnology in fiber finishing. Synth Fibers .32(1): 20–22.

21. Parta. JK, Gouda S (2013) Application of nanotechnology in textile engineering: A review. JETR (5): 104–111

22. Salama, D. M., Osman, S. A., Abd El-Aziz, M. E., Abd Elwahed, M. S., & Shaaban, E. A. (2019). Effect of zinc oxide nanoparticles on the growth, genomic DNA, production and the quality of common dry bean (Phaseolus vulgaris). Biocatalysis and Agricultural Biotechnology, 18, 101083.

23. Youssef AM, Abou-Yousef H, El-Sayed SM, Kamel S (2015) Mechanical and antibacterial properties of novel high-performance chitosan/nanocomposite films. International Journal of Biological Macromolecules 76, 25–32

24. Noah, A. Z., El Semary, M. A, Youssef, A. M and El- Safty M. A. Enhancement of Yield point at High pressure High temperature wells by using Polymer nanocomposites based on Zinc oxide& Calcium carbonate nanoparticles. Egyptian Journal of Petroleum, 26 (2017), 33-40

25. Youssef, A.M. Morphological studies of polyaniline nanocomposite based Mesostructured TiO$_2$ nanowires as conductive packaging materials, RSC Advances, 4 (2014) 6811–6820.

26. Youssef AM, Malhat FM (2014) Selective Removal of Heavy Metals from Drinking Water Using Titanium Dioxide Nanowire, Macromol. Symp., 337, 96–101.

27. El-Sayed NS, El-Sakhawy M, Brun N, Hesemann P, Kamel S (2018) New approach for immobilization of 3-aminopropyltrimethoxysilan into cellulose and hybrid formation with TiO$_2$ as scaffold for human BJ1 proliferation. Carbohydrate Polymers, 199 193–204.

28. Moustafa H, Darwish NA, Youssef AM, Reda S, El-Wakil AA (2018) High-Performance of Nanoparticles and Their Effects on the Mechanical, Thermal Stability and UV Shielding Properties of PMMA Nanocomposites. Egypt. J. Chem., 61, 23 - 32.

29. Kamel S (2012) Rapid synthesis of antimicrobial paper under microwave irradiation. Carbohydrate Polymers (90) 1538– 1542.

30. StephanT, Panittamat K and Pranut P (2006) Layer by layer deposition of antimicrobial silver nanoparticles on textile fibers. Colloids Surf A 2(89): 105–109

31. Muralidhara KS, Sreenivasan S (2012) Adaptation of pyrolytic conduit of polyester cotton blended fabric with flame retardant chemical concentrations. J Chem Sci. (2) 20–25).

32. Youssef, A.M., El-Sayed, S.M., El-Sayed, H.S., ...Assem, F.M., Abd El-Salam, M.H.Novel bionanocomposite materials used for packaging

_____

_____

skimmed milk acid coagulated cheese (Karish) International Journal of Biological Macromolecules, 2018, 115, pp. 1002-1011

33. Youssef, A.M., Malhat, F.M., Abd El-Hakim, A.F.A. Preparation and Utilization of Polystyrene Nanocomposites Based on TiO2 Nanowires. Polymer - Plastics Technology and Engineering, 2013, 52(3), pp. 228-235

34. Khattab T A, Abou-Yousef H, and Kamel S (2018) Photoluminescent spray-coated paper sheet: Write-in-the-dark. Carbohydrate Polymers, 200, 154–161

35. Dacrory S, Abou-Yousef H, Abouzeid RE, Kamel S, Abdel-aziz M S, Elbadry M. Antimicrobial cellulosic hydrogel from olive oil industrial residue. International Journal of Biological Macromolecules, 25 May 2018, 117:179-188

36. Emandi A, Vasiliu C, Budrugeac P, Stamatin I (2011) Quantitative investigation of wood composition by integrated FT-IR and thermogravimetric methods-cellulose chemistry and technology –vol.3 No (6) ,223-243

37. Inari GN, Petrissans M, Gerardin P (2007) Chemical reactivity of heat-treated wood, Wood Science and Technology, Volume 41, no.2, 157-168(12). 245.

38. Bakar B, Hiziroglu S, Tahir. P. (2013) Properties of some thermally modified wood species. Materials and Design 43: 348-355.

39. El-Ebissy AA, Michael MN, Shady KE (2016) Effect of nano zinc oxide on the structural characteristic, tensile thermal properties of textile fabrics, Journal of Industrial Textiles 46(1) 130–142.

_____